Validation of the finite-volume quantization condition for two spinless particles

Frank Lee, Andrei Alexandru, Ruairí Brett
George Washington University

Lattice 2021 virtual meeting (MIT), 27 July 2021

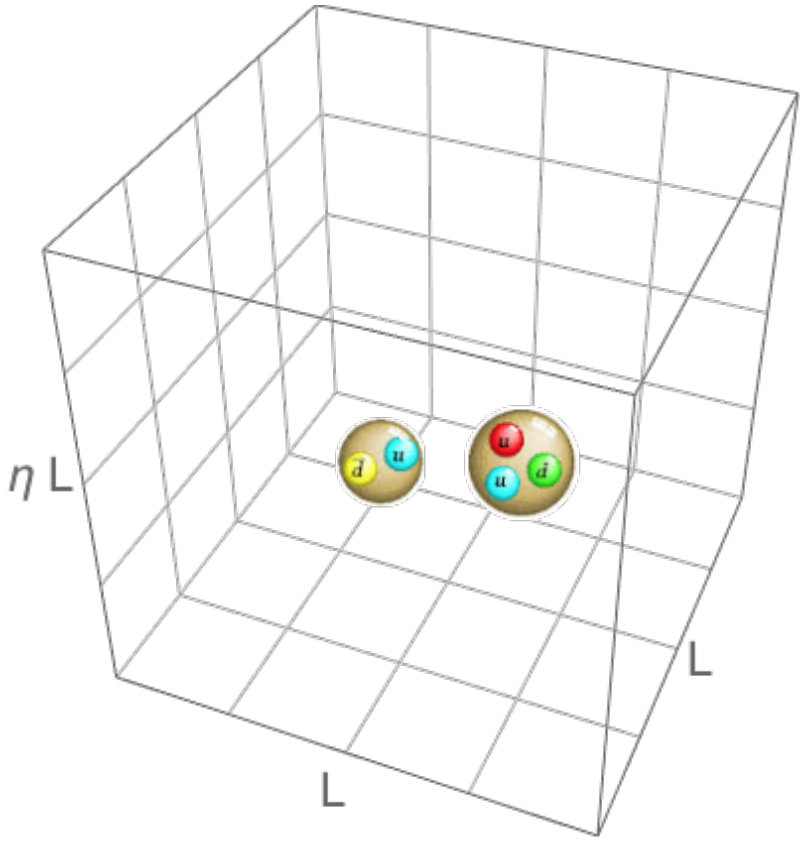

Lüscher method

Infinite volume,

- Finite interaction range R
- Phaseshift is introduced in the asymptotic region (r>R) to characterize the interaction

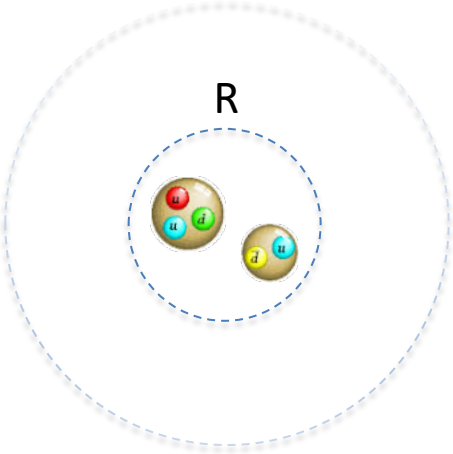

Finite box of size L,

- Periodic boundary conditions
- Require L>2R

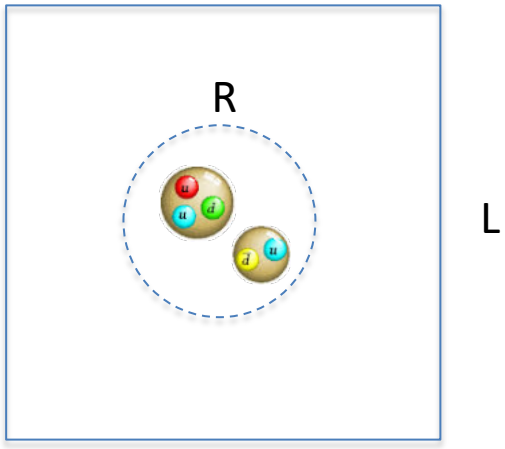

Lüscher established an exact relation between elastic scattering phaseshift in the infinite volume and discrete interaction energy levels in the box.

It does not matter how the interaction energy is obtained in the box,

- Lattice QCD in terms of quark-gluon dynamics
- Or effective field theories
- Or quantum mechanics

Quantization Condition

$$\prod_{\Gamma} \det\left[M^{\Gamma}_{J,J'}(k,L) - \delta_{JJ'} \cot\delta_J(k) \right] = 0$$

Γ = irreducible representations of a symmetry group
L = box size
k = discrete box levels
δ_J(k) = infinite-volume phaseshifts

Each QC is a single condition that couples to an infinite tower of angular momenta. Only the lowest phaseshift can be predicted.

$$\det\begin{pmatrix} M_{11}-\cot\delta_{J1} & M_{12} & \cdots \\ M_{21} & M_{22}-\cot\delta_{J2} & \cdots \\ \cdots & \cdots & \ddots \end{pmatrix} = 0$$

How to validate ?

1) Compute δ_J(k) from an interaction model
2) Compute k in a box from the same interaction
3) Use δ_J(k) as input, solve for k and compare with box levels
4) Enlarge QC order by order: order 1= lowest J, order 2= lowest two Js, order 3= lowest 3 Js, etc
5) Better agreement is expected as the order is increased.

Example:
Matrix elements up to l=5 for rest frame d=(0,0,0) in cubic box (group Oh).

$$\prod_{\Gamma} \det\left[\mathcal{M}^{\Gamma}_{J,J'} - \delta_{JJ'}\cot\delta_J\right] = 0$$

$$W_{lm} = \frac{\mathcal{Z}_{lm}(q^2, L)}{\pi^{3/2} q^{l+1}}, \quad q = k\frac{L}{2\pi}$$

$$\mathcal{Z}_{lm} = \sum_{n=\{n_1,n_2,n_3\}\in Z^3} \frac{n^l Y_{lm}(\theta,\phi)}{n^2 - q^2} \left(\text{zeta function}\right)$$

Γ	l	n	l'	n'	$M^{\Gamma}_{ln,l'n'}$
A_{1g}	0	1	0	1	w_{00}
	0	1	4	1	$2\sqrt{\frac{3}{7}}w_{40}$
	4	1	4	1	$w_{00} + \frac{108w_{40}}{143} + \frac{80w_{60}}{11\sqrt{13}} + \frac{560w_{80}}{143\sqrt{17}}$
A_{2u}	3	1	3	1	$w_{00} - \frac{12w_{40}}{11} + \frac{80w_{60}}{11\sqrt{13}}$
E_g	2	1	2	1	$w_{00} + \frac{6w_{40}}{7}$
	2	1	4	1	$-\frac{40}{77}\sqrt{3}w_{40} - \frac{30}{11}\sqrt{\frac{3}{13}}w_{60}$
	4	1	4	1	$w_{00} + \frac{108w_{40}}{1001} - \frac{64w_{60}}{11\sqrt{13}} + \frac{392w_{80}}{143\sqrt{17}}$
E_u	5	1	5	1	$w_{00} + \frac{1152\sqrt{21}w_{100}}{4199} - \frac{6w_{40}}{13} + \frac{32w_{60}}{17\sqrt{13}} - \frac{672w_{80}}{247\sqrt{17}}$
T_{1g}	4	1	4	1	$w_{00} + \frac{54w_{40}}{143} - \frac{4w_{60}}{11\sqrt{13}} - \frac{448w_{80}}{143\sqrt{17}}$
T_{1u}	1	1	1	1	w_{00}
	1	1	3	1	$-\frac{4w_{40}}{\sqrt{21}}$
	1	1	5	1	$\frac{5w_{40}}{\sqrt{33}} + 6\sqrt{\frac{3}{143}}w_{60}$
	1	1	5	2	$\sqrt{\frac{15}{77}}w_{40} - 2\sqrt{\frac{105}{143}}w_{60}$
	3	1	3	1	$w_{00} + \frac{6w_{40}}{11} + \frac{100w_{60}}{33\sqrt{13}}$
	3	1	5	1	$-\frac{60w_{40}}{13\sqrt{77}} - \frac{7}{3}\sqrt{\frac{7}{143}}w_{60} - \frac{56}{13}\sqrt{\frac{7}{187}}w_{80}$
	3	1	5	2	$\frac{12}{13}\sqrt{\frac{5}{11}}w_{40} - 7\sqrt{\frac{5}{143}}w_{60} - \frac{56}{39}\sqrt{\frac{5}{187}}w_{80}$
	5	1	5	1	$w_{00} + \frac{756\sqrt{21}w_{100}}{4199} + \frac{6w_{40}}{13} + \frac{80w_{60}}{51\sqrt{13}} + \frac{490w_{80}}{247\sqrt{17}}$
	5	1	5	2	$-\frac{2772\sqrt{\frac{3}{5}}w_{100}}{4199} + \frac{6}{13}\sqrt{\frac{5}{7}}w_{40} + \frac{8}{17}\sqrt{\frac{35}{13}}w_{60} - \frac{154}{741}\sqrt{\frac{35}{17}}w_{80}$
	5	2	5	2	$w_{00} - \frac{84\sqrt{21}w_{100}}{323} - \frac{6w_{40}}{13} + \frac{32w_{60}}{17\sqrt{13}} + \frac{14\sqrt{17}w_{80}}{247}$
T_{2g}	2	1	2	1	$w_{00} - \frac{4w_{40}}{7}$
	2	1	4	1	$\frac{20\sqrt{3}w_{40}}{77} - \frac{40}{11}\sqrt{\frac{3}{13}}w_{60}$
	4	1	4	1	$w_{00} - \frac{54w_{40}}{77} + \frac{20w_{60}}{11\sqrt{13}}$
T_{2u}	3	1	3	1	$w_{00} - \frac{2w_{40}}{11} - \frac{60w_{60}}{11\sqrt{13}}$
	3	1	5	1	$\frac{20w_{40}}{13\sqrt{11}} + \frac{14w_{60}}{\sqrt{143}} - \frac{112w_{80}}{13\sqrt{187}}$
	5	1	5	1	$w_{00} - \frac{432\sqrt{21}w_{100}}{4199} + \frac{4w_{40}}{13} - \frac{80w_{60}}{17\sqrt{13}} - \frac{280w_{80}}{247\sqrt{17}}$

Cubic vs. Elongated symmetry

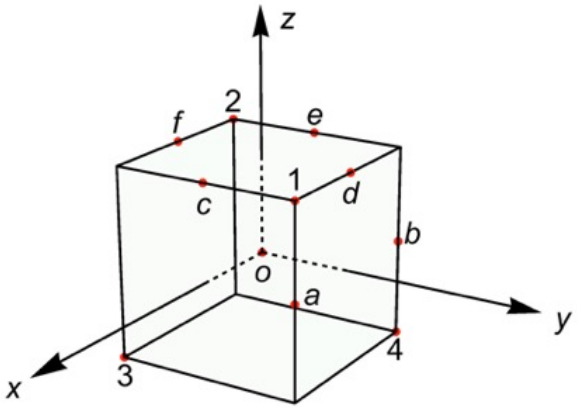

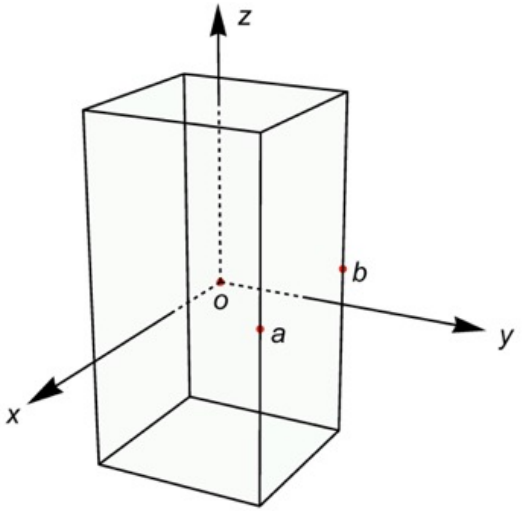

Angular momentum decomposition in box geometry for rest and moving frames

O_h		D_{4h}		C_{4v}		C_{3v}		C_{2v}		C_{1v}	
Γ	l	Γ	l	Γ	l	Γ	l	Γ	l	Γ	l
A_{1g}	$0,4,6$	A_{1g}	$0,2,4(2),5$	A_1	$0,1,2,3,4(2)$	A_1	$0,1,2,3(2),4(2)$	A_1	$0,1,2(2),3(2),4(3)$	A_1	$0,1(2),2(3),3(4)$
A_{1u}	$9,13,15$	A_{1u}	$5,7,9(2)$								
A_{2g}	$6,10,12$	A_{2g}	$4,6,8(2)$	A_2	$4,5,6$	A_2	$3,4,5$	A_2	$2,3,4(2),5(2)$	$A2$	$1,2(2),3(3),4(4)$
A_{2u}	$3,7,9$	A_{2u}	$1,3,5(2),7(2)$								
E_g	$2,4,6$	E_g	$2,4(2),6(3)$	E	$1,2,3(2),4(2)$	E	$1,2(2),3(2),4(3)$				
E_u	$5,7,9$	E_u	$1,3(2),5(3)$								
T_{1g}	$4,6,8(2)$	B_{1g}	$2,4,6(2),8(2)$	B_1	$2,3,4,5$			B_1	$1,2,3(2),4(2),5(3)$		
T_{1u}	$1,3,5(2)$	B_{1u}	$3,5,7(2),9(2)$								
T_{2g}	$2,4,6(2)$	B_{2g}	$2,4,6(2),8(2)$	B_2	$2,3,4,5$			B_2	$1,2,3(2),4(2),5(3)$		
T_{2u}	$3,5,7(2)$	B_{2u}	$3,5,7(2),9(2)$								

Lowest partial wave in each irrep can be predicted by Lüscher method.

Scattering in infinite volume

Phaseshift can be obtained in the CM frame,

$$E = \frac{\hbar^2 k^2}{2\mu}$$

$$H = -\frac{\hbar^2}{2\mu}\nabla^2 + V(r) \qquad \left[-\frac{\hbar^2}{2\mu}\frac{d^2}{dr^2} + \frac{l(l+1)\hbar^2}{2\mu r^2} + V(r)\right] u_l(r) = E u_l(r)$$

$$\lim_{r\to 0} u_l(r) = 0 \quad \text{and} \quad \lim_{r\to\infty} u_l(r) \propto e^{i\delta_l(k)} \sin\left[kr - \frac{l\pi}{2} + \delta_l(k)\right]$$

Simple test potential,

$m_1 = 0.138$ GeV, $m_2 = 0.94$ GeV

$V(r) = C\, e^{-\frac{1}{2}\left(\frac{r}{R_0}\right)^2}$

$C = 1.0$ GeV, $R_0 = 1.25$ fm

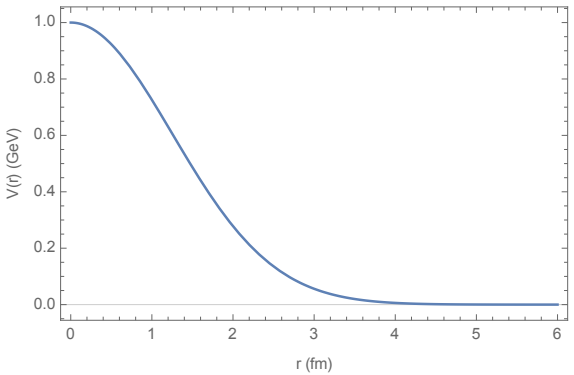

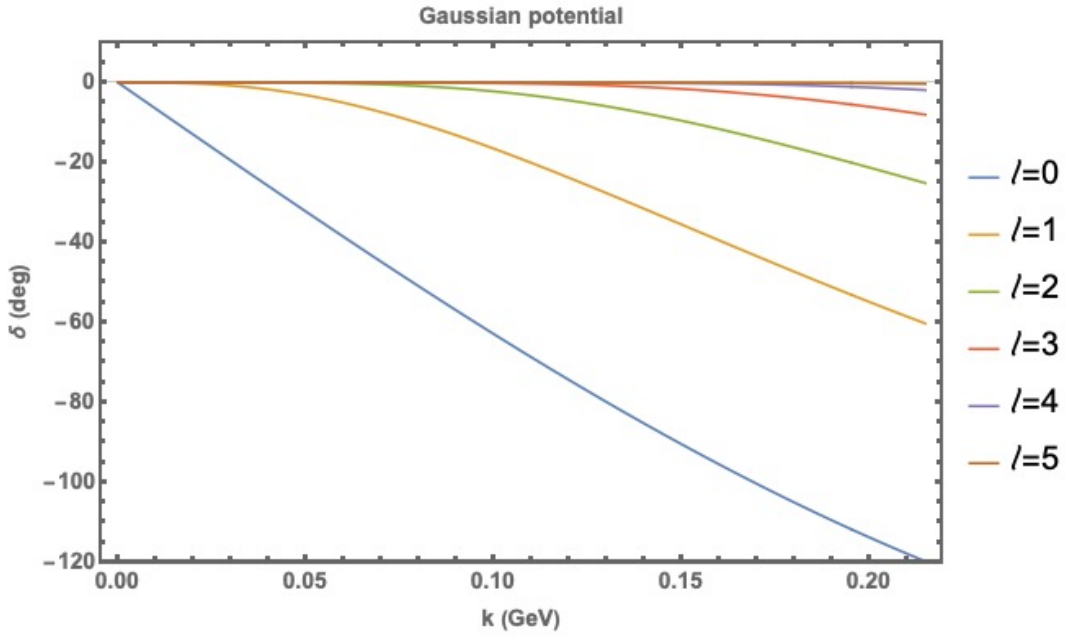

Since the range R=4 fm, we use a box of L=24 fm.

Lattice Hamiltonian

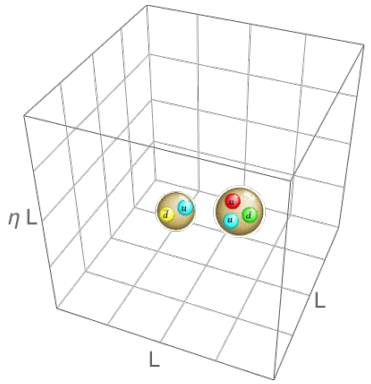

$$H|\psi\rangle = E|\psi\rangle \qquad H = -\frac{\hbar^2}{2m_1}\nabla_1^2 - \frac{\hbar^2}{2m_2}\nabla_2^2 + V\left(|\vec{r}_1 - \vec{r}_2|\right)$$

Total momentum of the two-particle system in the lab frame: $P=p_1+p_2$.

It can be solved directly by discretizing it on the lattice ($V=N_x x N_y x N_z$, spacing a)

- 6-dimentional problem (x_1, y_1, z_1, x_2, y_2, z_2)
- Laplacian operator is approximated by finite differences
- $N^6 x N^6$ eigensystem
- Only feasible for small lattices
- Useful for checking purposes

$$P = \frac{2\pi}{L} d = \frac{2\pi}{a}\left(\frac{i}{N_x}, \frac{j}{N_y}, \frac{k}{N_z}\right)$$

$$i = 0,1,2,\ldots,N_x - 1$$

$$j = 0,1,2,\ldots,N_y - 1$$

$$k = 0,1,2,\ldots,N_z - 1$$

For N=4 lattice,

- Full spectrum has 4096 eigenvalues and eigenvectors.
- They can be separated into 64 sectors of P, each sector having 64 states.
- The separation can be realized uniquely by constructing common eigenvectors of commuting operators {H, pxsin, pxcos, pysin, pycos, pzsin, pzcos}.

$$\mathrm{Sin}(P_x a) = \frac{T_x - T_x^\dagger}{2i}$$

$$\mathrm{Cos}(P_x a) = \frac{T_x + T_x^\dagger}{2}$$

Translation operator $T_x = e^{iP_x a}$

Reduction of lattice Hamiltonian

The two-particle Hamiltonian can be expressed in Fock-space number representation $|n_1,n_2\rangle$ in terms of creation and annihilation operators,

$$H = -\frac{\hbar^2}{2m_1 a^2}\sum_{n_1}\left[a^\dagger(n_1)a(n_1+1)+a^\dagger(n_1)a(n-1_1)-2a^\dagger(n_1)a(n_1)\right]$$

$$-\frac{\hbar^2}{2m_2 a^2}\sum_{n_2}\left[a^\dagger(n_2)a(n_2+1)+a^\dagger(n_2)a(n_2-1)-2a^\dagger(n_2)a(n_2)\right]+\sum_{n_1,n_2}V(n_1,n_2)a^\dagger(n_1)a(n_1)a^\dagger(n_2)a(n_2)$$

It can be projected onto a basis of fixed total momentum P and relative coordinate r, given in 3-stencil form

$$\left|P,r\right\rangle = \sum_m e^{iPm}\left|m,m+r\right\rangle$$

$$H\left|P,r\right\rangle = -\frac{\hbar^2}{2a^2}\left[\left(\frac{e^{iP}}{m_1}+\frac{1}{m_2}\right)\left|P,r+1\right\rangle+\left(\frac{e^{-iP}}{m_1}+\frac{1}{m_2}\right)\left|P,r-1\right\rangle-2\left(\frac{1}{m_1}+\frac{1}{m_2}\right)\left|P,r\right\rangle\right]+V(r)\left|P,r\right\rangle+O(a^2)$$

If P=0, it reduces to the standard form,

$$H\left|r\right\rangle = -\frac{\hbar^2}{2\mu a^2}\left[\left|r+1\right\rangle+\left|r-1\right\rangle-2\left|r\right\rangle\right]+V(r)\left|r\right\rangle$$

which coincides with the form in CM frame.

Main advantages of this formalism:

1) It is a N^3 eigenvalue problem (instead of N^6 in the unprojected $|n_1,n_2\rangle$ basis). We can obtain the full spectrum quickly for lattices up to 32^3 on a desktop computer.
2) Working in the lab frame
3) Moving frames (non-zero P) are naturally described (P is an input)

In practice, we use an improved version from a centered 7-point stencil for fast convergence,

$$H=-\frac{\hbar^2}{2}\sum_{j=x,y,z}\frac{-1}{180a^2}\left[-2\left(\frac{e^{3iP_j}}{m_1}+\frac{1}{m_2}\right)\left|P_j,j+3\right\rangle+27\left(\frac{e^{2iP_j}}{m_1}+\frac{1}{m_2}\right)\left|P_j,j+2\right\rangle-270\left(\frac{e^{iP_j}}{m_1}+\frac{1}{m_2}\right)\left|P_j,j+1\right\rangle\right.$$

$$\left.-2\left(\frac{e^{-3iP_j}}{m_1}+\frac{1}{m_2}\right)\left|P_j,j-3\right\rangle+27\left(\frac{e^{-2iP_j}}{m_1}+\frac{1}{m_2}\right)\left|P_j,j-2\right\rangle-270\left(\frac{e^{-iP_j}}{m_1}+\frac{1}{m_2}\right)\left|P_j,j-1\right\rangle+490\left(\frac{1}{m_1}+\frac{1}{m_2}\right)\left|P_j,j\right\rangle\right]$$

$$+V(x,y,z)\left|P,x,y,z\right\rangle+O(a^6)$$

3-point stencil,

$$H\left|P,r\right\rangle=-\frac{\hbar^2}{2a^2}\left[\left(\frac{e^{iP}}{m_1}+\frac{1}{m_2}\right)\left|P,r+1\right\rangle+\left(\frac{e^{-iP}}{m_1}+\frac{1}{m_2}\right)\left|P,r-1\right\rangle-2\left(\frac{1}{m_1}+\frac{1}{m_2}\right)\left|P,r\right\rangle\right]+V(r)\left|P,r\right\rangle+O(a^2)$$

Energy levels in a cubic box of L=24 fm, projected into irreps of Oh.

$$\lim_{\substack{a\to 0 \\ N\to\infty}} Na = L$$

Box levels are obtained by continuum extrapolation using lattices 20^3 at a=1.2 fm, 24^3 at a=1.0 fm, 30^3 at a=0.8 fm.

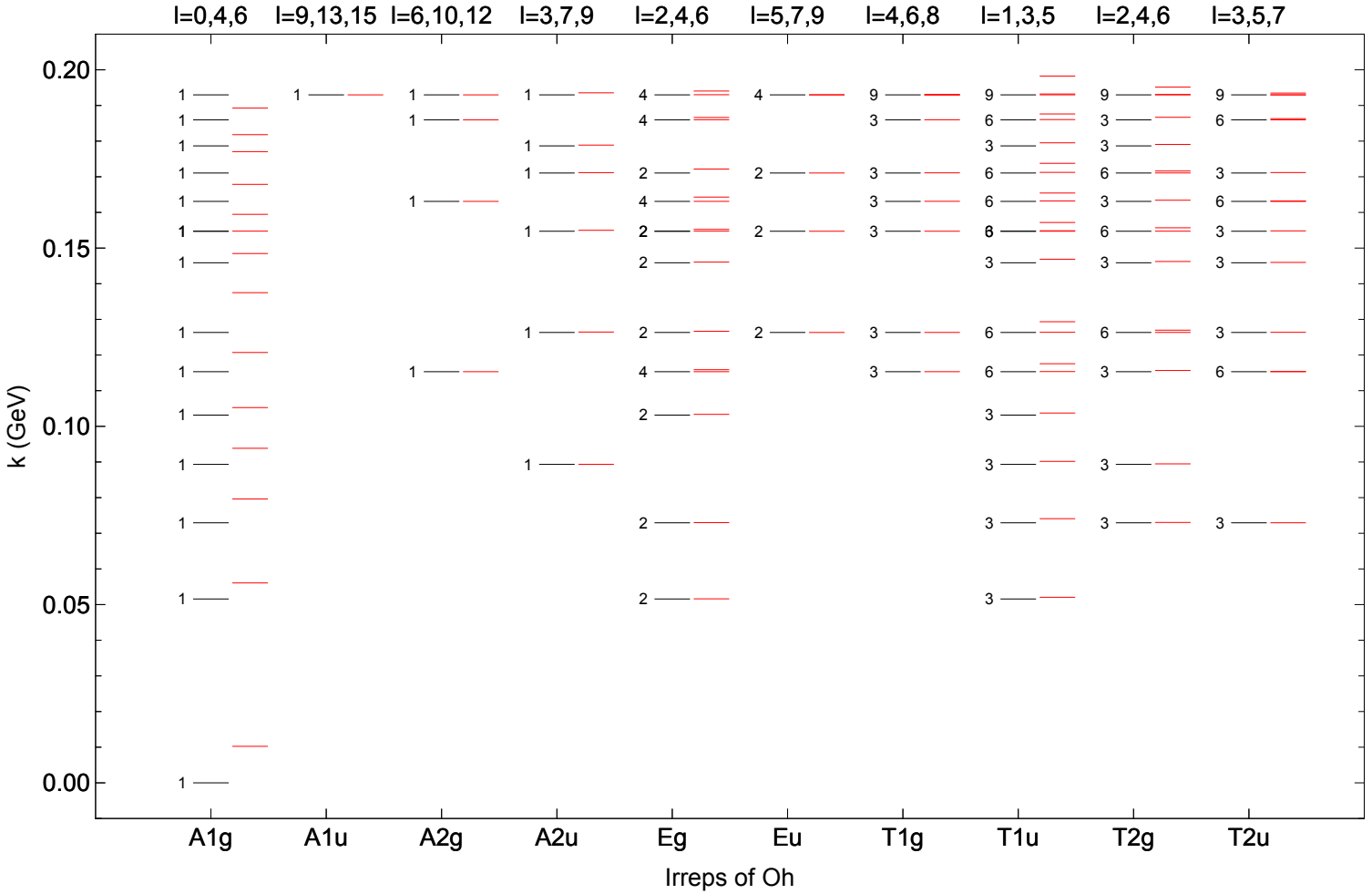

$$E = \frac{\hbar^2 k^2}{2\mu}$$

black: free particles (with degeneracies)

red: interacting particles

Phaseshift reconstruction in cubic (left) and elongated (right) boxes.

Blue curves: infinite-volume $\delta_J(k)$
Black points: finite volume $\delta_J(k)$
Faint vertical lines: free-particle poles

1) Feed the box levels k to QC to predict lowest $\boldsymbol{\delta}$ and compare with infinite-volume values.

2) Phaseshift largely reconstructed up to k=0.2 GeV

3) Exceptions are observed. They happen at free-particle poles (pinching).

4) Higher partial waves?

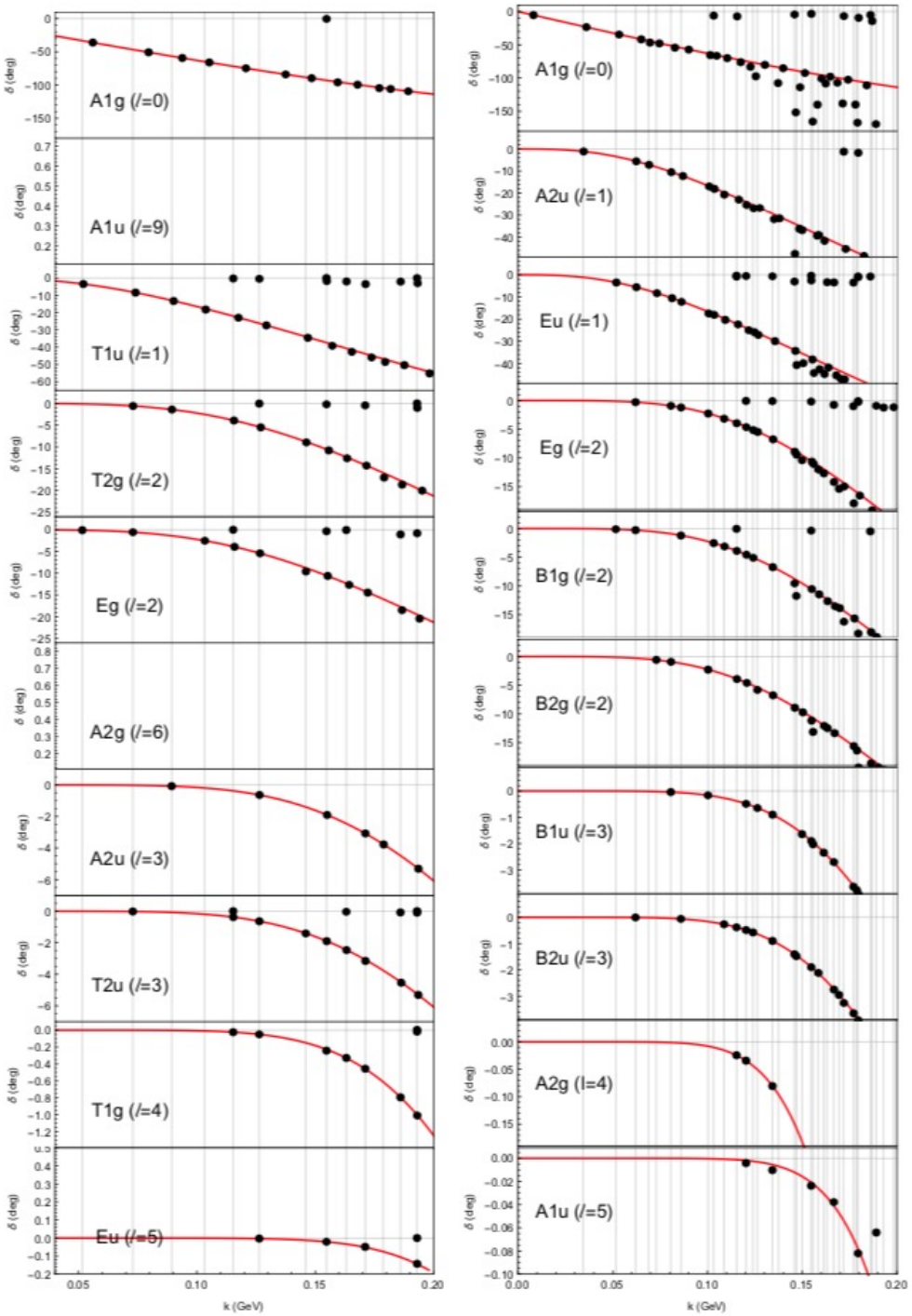

Convergence of QC

$$T_1^-:\ \det\begin{pmatrix} M_{11}-\cot\delta_1(k) & M_{13} & \cdots \\ M_{31} & M_{33}-\cot\delta_3(k) & \cdots \\ \cdots & \cdots & \ddots \end{pmatrix}=0$$

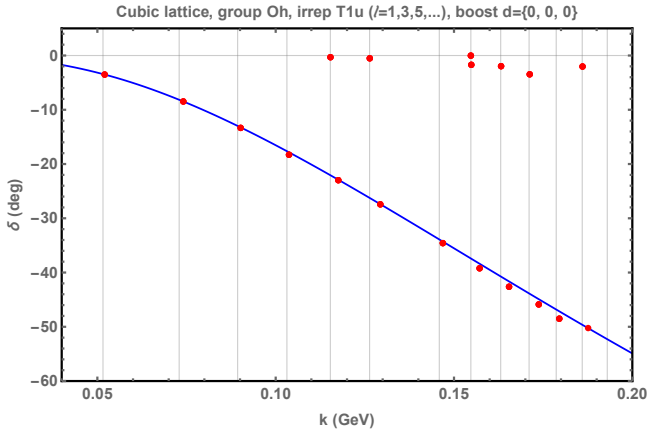

chi-square measure:

$$\chi^2=\frac{\left(k_{box}-k_{QC}\right)^2}{\left(k_{box}-k_{lat}\right)^2}$$

k_{box} = box levels
k_{lat} = levels from largest lattice
k_{QC} = roots from QC at each orde
* = free-particle poles

Convergence indicates high-precision validation of QC.

Level	Box L	Lattice	Order 1	Order 2	Order 3	χ^2 Order 1	χ^2 Order 2	χ^2 Order 3
22	0.198249	0.198241	0.198146	0.198245	0.19825	167.097	0.249283	0.0101593
21	0.193217	0.193213	*0.192974	0.193209	0.193221	2998.88	3.71223	0.470423
20	0.192982	0.192978	*0.192974	*0.192974	0.192975	3.26057	3.26057	2.49916
19	0.187618	0.187613	0.187614	0.187615	0.187619	0.747838	0.42273	0.00535232
18	0.186043	0.186039	*0.185954	0.186041	0.186045	389.699	0.356124	0.194373
17	0.179522	0.179521	0.179489	0.179517	0.179522	807.378	17.3011	0.0125204
16	0.173768	0.173763	0.173698	0.173767	0.173769	206.536	0.0359251	0.00582583
15	0.171233	0.171228	*0.171053	0.171231	0.171233	1447.64	0.209609	0.00394721
14	0.165438	0.165434	0.165382	0.165438	0.165439	128.455	0.0154137	0.00520841
13	0.163206	0.163201	*0.163093	0.163204	0.163206	526.933	0.147073	0.0123243
12	0.157179	0.157177	0.157134	0.157178	0.157179	551.783	0.156363	0.00460883
11	0.154856	0.154853	*0.154723	0.154856	0.154857	1267.98	0.0467443	0.00685293
10	0.154726	0.154725	*0.154723	*0.154723	0.154726	6.59657	6.59657	0.0176498
9	0.146868	0.146867	0.14686	0.146867	0.146868	172.894	2.71263	0.0020146
8	0.129339	0.129339	0.129335	0.129339	0.129339	58.3417	0.000653416	0.0113939
7	0.126379	0.126379	*0.126331	0.126379	0.126379	30130.9	0.976735	0.00253806
6	0.11756	0.117559	0.117552	0.11756	0.11756	323.653	0.0133041	0.00803915
5	0.115359	0.115359	*0.115324	0.115359	0.115359	13893.6	0.272455	0.002095
4	0.103734	0.103734	0.10372	0.103734	0.103734	1539.04	0.0089603	0.0024343
3	0.0901719	0.0901719	0.0901658	0.0901719	0.0901719	11790.7	0.0587094	0.0204841
2	0.0740985	0.0740985	0.0740982	0.0740985	0.0740985	27.9224	0.011686	0.0285701
1	0.0520501	0.0520501	0.0520494	0.0520501	0.0520501	836.425	0.0286906	0.0308669
					Total χ^2	**67276.5**	**36.5936**	**3.35684**

Sensitivity to second partial wave

$$\cot\delta_{2nd} = M_{22} + \frac{|M_{12}|^2}{\cot\delta_{1st} - M_{11}}$$

`Pinched' points give phaseshift predictions for the 2nd partial wave.

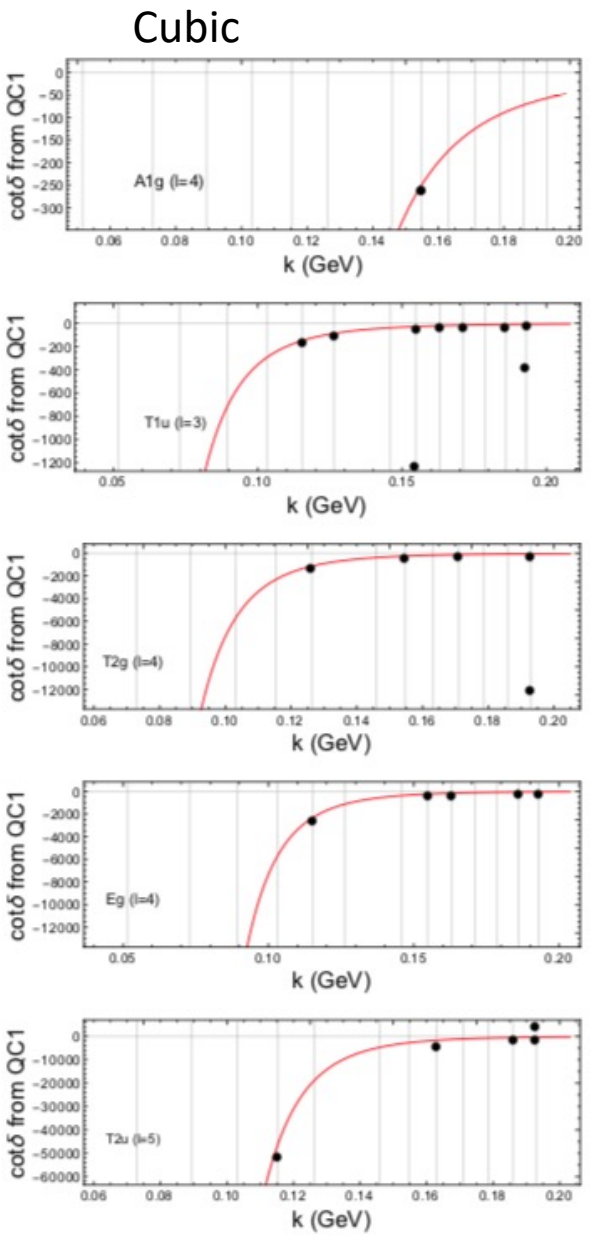

FIG. 14. Second partial waves in rest frame of cubic box. The black points are $\cos\delta_{2nd}$ in Eq.(61) with $\cos\delta_{1st}$ neglected, evaluated at the pinched box levels from order 1. The red curves are the infinite-volume values for $\cos\delta_{2nd}$. The faint vertical lines are the free-particle levels.

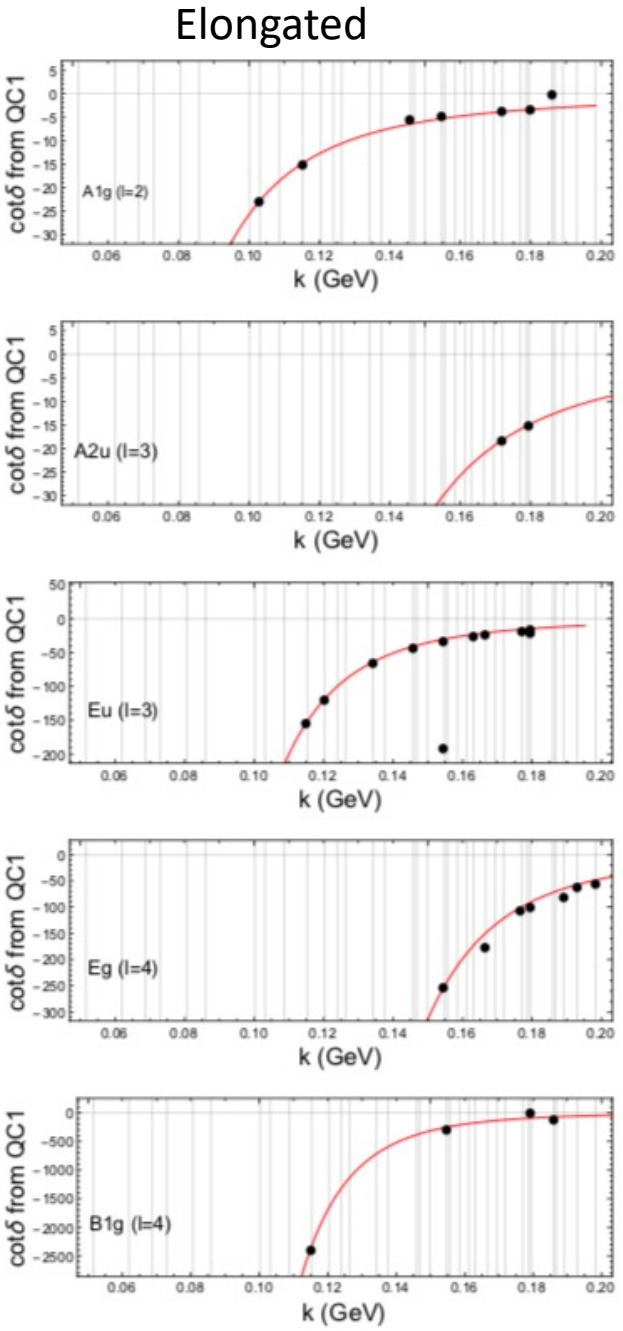

FIG. 15. Second partial waves in rest frame of elongated box.

Conclusion

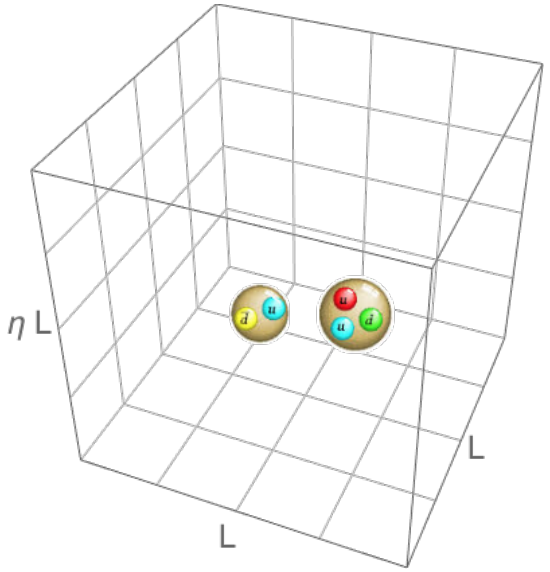

- We validated with high precision 45 QCs up to J=4 (some 5) for two spinless particles of unequal masses.
  - they are safe to use
- We found sensitivity to 2nd partial wave.
- Details can be found in
  - https://arxiv.org/abs/2107.04430

Cubic box

No.	d	Group	QC	$l(n)$	N	Order 1	Order 2	Order 3	Order 4	Order 5
1	(0, 0, 0)	O_h	A_{1g}	$0, 4, 6, \cdots$	14	277.206	3.7296			
			A_{1u}	$9, 13, 15, \cdots$						
			A_{2g}	$6, 10, 12, \cdots$						
2			A_{2u}	$3, 7, 9, \cdots$	6	0.0458813				
3			E_g	$2, 4, 6, \cdots$	16	2123.07	5.44639			
4			E_u	$5, 7, 9, \cdots$	5	0.0546959				
5			T_{1g}	$4, 6, 8(2), \cdots$	9	0.243897				
6			T_{1u}	$1, 3, 5(2), \cdots$	22	67276.5	36.5936	3.35684		
7			T_{2g}	$2, 4, 6(2), \cdots$	16	2485.36	2.70125			
8			T_{2u}	$3, 5, 7(2), \cdots$	14	4.55575	0.267262			
10	(0, 0, 1)	C_{4v}	A_1	$0, 1, 2, 3, 4(2), \cdots$	40	4.08008×10^8	1.06106×10^{20}	10175.7	284.022	6.92792
11			A_2	$4, 5, 6, \cdots$	15	7.46202	0.145375			
12			B_1	$2, 3, 4, 5, \cdots$	34	276889.	402.025	5.9668		
13			B_2	$2, 3, 4, 5, \cdots$	27	350956.	779.183	3.84012		
14			E	$1, 2, 3(2), 4(2), \cdots$	40	1.32751×10^7	72379.5	514.979	8.21687	
14	(1, 1, 0)	C_{2v}	A_1	$0, 1, 2(2), 3(2), 4(3), \cdots$	40	1.96654×10^8	4.77126×10^6	17298.1	190.94	5.34113
15			A_2	$2, 3, 4(2), 5(2), \cdots$	40	54211.3	2998.61	3.01327		
16			B_1	$1, 2, 3(2), 4(2), \cdots$	40	2.84806×10^6	47754.8	241.517	4.62961	
17			B_2	$1, 2, 3(2), 4(2), \cdots$	40	9.36978×10^6	88719.7	308.013	6.28652	
18	(1, 1, 1)	C_{3v}	A_1	$0, 1, 2, 3(2), 4(2), \cdots$	40	9.16556×10^7	1.09895×10^6	22260.	115.412	3.53446
19			A_2	$3, 4, 5, \cdots$	26	111.322	0.44229			
20			E	$1, 2(2), 3(2), 4(3), \cdots$	40	8.06257×10^6	23959.	271.289	4.13508	
21	(0, 1, 2)	C_{1v}	A_1	$0, 1(2), 2(3), 3(4), 4(5), \cdots$	40	1.01852×10^8	993629.	6858.3	17.3429	2.01417
22			A_2	$1, 2(2), 3(3), 4(4), \cdots$	40	8.98645×10^6	37314.8	293.484	3.18387	

Elongated box

No.	d	Group	QC	$l(n)$	N	Order 1	Order 2	Order 3	Order 4	Order 5
23	(0, 0, 0)	D_{4h}	A_{1g}	$0, 2, 4(2), 5, \cdots$	40	4.06688×10^6	573.449	8.64225		
24			A_{1u}	$5, 7, 9(2), \cdots$	9	0.134224				
25			A_{2g}	$4, 6, 8(2), \cdots$	3	0.00828583				
26			A_{2u}	$1, 3, 5(2), 7(2), \cdots$	34	131946.	16.2795	10.7998		
27			E_g	$2, 4(2), 6(3), \cdots$	38	2009.93	0.319341			
28			E_u	$1, 3(2), 5(3), \cdots$	40	221693.	41.2595	8.52709		
29			B_{1g}	$2, 4, 6(2), 8(2), \cdots$	27	703.291	11.0395			
30			B_{1u}	$3, 5, 7(2), 9(2), \cdots$	17	7.07159	0.168506			
31			B_{2g}	$2, 4, 6(2), 8(2), \cdots$	22	2093.46	0.192			
32			B_{2u}	$3, 5, 7(2), 9(2), \cdots$	21	2.06599	0.488025			
33	(0, 0, 1)	C_{4v}	A_1	$0, 1, 2, 3, 4(2), \cdots$	40	5.70458×10^8	9.64404×10^6	14025.4	166.777	11.0137
34			A_2	$4, 5, 6, \cdots$	21	40.092	0.21509			
35			B_1	$2, 3, 4, 5, \cdots$	40	161200.	274.945	5.1077		
36			B_2	$2, 3, 4, 5, \cdots$	39	318459.	845.868	2.82798		
37			E	$1, 2, 3(2), 4(2), \cdots$	40	1.66366×10^7	79648.3	353.966	7.28402	
38	(1, 1, 0)	C_{2v}	A_1	$0, 1, 2(2), 3(2), 4(3), \cdots$	40	2.19334×10^8	3.60527×10^6	9669.56	99.3024	27.4093
39			A_2	$2, 3, 4(2), 5(2), \cdots$	40	34211.4	295.311	0.804797		
40			B_1	$1, 2, 3(2), 4(2), \cdots$	40	2.97904×10^6	28179.	115.601	6.80754	
41			B_2	$1, 2, 3(2), 4(2), \cdots$	40	9.05592×10^6	71558.8	146.885	18.7042	
42	(1, 1, 1)	C_{1v}	A_1	$0, 1(2), 2(3), 3(4), 4(5), \cdots$	40	5.45564×10^8	2.89417×10^6	15983.3	39.1208	8.00598
43			A_2	$1, 2(2), 3(3), 4(4), \cdots$	40	6.85779×10^6	23813.9	69.434	3.24328	
44	(0, 1, 2)	C_{1v}	A_1	$0, 1(2), 2(3), 3(4), 4(5), \cdots$	40	3.79138×10^8	3.16621×10^6	6213.69	17.0296	5.34524
45			A_2	$1, 2(2), 3(3), 4(4), \cdots$	40	1.27375×10^7	45256.8	146.374	2.67257	